Efficient Type II Phase-Matching Second Harmonic Generation in Ba:Yb:Nb:RbTiOPO$_4$/RbTiOPO$_4$ waveguides

J. Cugat, R. Solé*, J.J. Carvajal, X. Mateos, M.C. Pujol, J. Massons, F. Díaz and M. Aguiló

Física i Cristal·lografia de Materials i Nanomaterials (FiCMA-FiCNA) and EMaS, Universitat Rovira i Virgili (URV),Campus Sescelades, C/Marcel·li Domingo s/n E-43007 Tarragona, Spain,
Corresponding author: rosam.sole@urv.cat

Efficient type-II phase-matching second harmonic generation of a 1125 nm fundamental beam has been obtained using Ba:Yb:Nb:RbTiOPO$_4$/RbTiOPO$_4$ waveguides grown by Liquid Phase Epitaxy. The refractive indices of the epitaxial layer have been measured at different wavelengths, and the Sellmeier coefficients of the chromatic dispersion curves have been obtained. The phase matching curve shows that the Ba^{2+} doping in RbTiOPO$_4$ contributes to increase the phase matching range until 900 nm. The experimental propagation modes agree well with the theoretical calculations.
    OCIS Codes: 190.0190, 310.0310, 230.0230

Rubidium titanyl phosphate, RbTiOPO$_4$ (RTP), is a nonlinear optical crystal that belongs to the KTiOPO$_4$ (KTP) family. It crystallizes in the orthorhombic space group *Pna2$_1$* [1]. This biaxial crystal has high nonlinear optical and electrooptical coefficients, which make it particularly useful for frequency doubling infrared laser radiation to obtain visible laser radiation [2]. More important, RTP presents high surface damage threshold (9.0 x 106 MW.m^{-2}) and large temperature matching bandwidth (50 K.cm^{-1}) which make of this material especially suitable for high power laser applications [3]. The incorporation of laser active ions, such as lanthanide (Ln^{3+}) ions, into the RTP structure is interesting for obtaining both emission and frequency doubling (self-frequency doubling, SFD) in the same crystal. By co-doping with Nb^{5+}, the Ln^{3+} concentration in these crystals has been demonstrated to be high enough for laser emission [4].

Of all the lanthanide ions, Yb^{3+} is of particular interest for emission at ~1 μm and the fact that it has a simple energy level scheme of only two energy levels, high absorption and emission cross sections, a low quantum defect, an absence of excited state absorption and a long lifetime.

Thus, epitaxial layers of Yb:Nb:RTP/RTP are interesting for fabricating compact and efficient laser sources in the IR and visible spectral regions by combining the emission (with large optical paths) and Second Harmonic Generation (SHG) processes with the waveguide structure that could be used in guided high power lasers. In a previous study, we probed the guiding of 532 nm and 632.8 nm laser radiation with TM polarization through RbTi$_{1-x-y}$Yb$_x$Nb$_y$OPO$_4$/RbTiOPO$_4$ epitaxial layers, but the contrast of refractive indices between the epilayer and the substrate was not large enough allow guiding of the light in the TE polarization [5].

The aim of this study is to obtain RTP epitaxial layers doped with Yb^{3+} and a contrast of refractive indices between the epilayer and the substrate high enough to allow the confinement of light in the TM and TE polarizations. According to the literature, introducing Ba^{2+} ions into the KTP structure increases of the refractive indices of the crystal [6]. Thus, we investigated the effect of Ba^{2+} in epitaxial layers of Yb:Nb:RTP/RTP grown by Liquid Phase Epitaxy (LPE). We measured the refractive indices of the substrate and the epilayer to predict theoretically the number of modes in the TE and TM polarizations that could be guided depending on the thickness of the epilayer. We found that the experimental propagation modes agreed well with our calculations. Finally, we studied the second harmonic radiation generated by type II birefringent phase-matching (PM) that was guided in these structures.

We used solutions containing WO$_3$ to grow Rb$_{1-x}$Ba$_x$Ti$_{1-y-z}$Yb$_y$Nb$_z$OPO$_4$ epitaxial layers by the LPE method. The solution composition was BaO·Rb$_2$O·P$_2$O$_5$·TiO$_2$·Nb$_2$O$_5$·Yb$_2$O$_3$·WO$_3$ = 0.88·43.02·23.61·20.70·0.45·1.35·10.00 (mol %) and its weight was about 80g. The thermal gradients in the solution were practically zero.

After the solution had been homogenized, we accurately determined its saturation temperature (Ts) and also studied the kinetics of the growth/dissolution at temperatures slightly above/below of the Ts. The substrates were 1.5 mm thick plates parallel to the (001) plane and were cut from RTP single crystals and polished down to an rms of 50·60 nm [7]. The (001) plane is of particular interest because it contains the direction of the type II birefringent PM ~1 μm, which includes the Yb^{3+} wavelength emission. The substrates, previously cleaned [8], were slowly introduced into the furnace to avoid thermal stresses and heated for about 1 h slightly above the solution surface. After that, they were dipped into the solution at a temperature of 1 K above the Ts to dissolve their surface slightly for 5 minutes. The next step was to decrease the temperature of the solution by 8 K below Ts to grow the epilayer for 5 h. During the whole process the substrate was rotated at 60 rpm. Finally, the substrate and the epilayer were removed from the solution and kept at a few mm above the surface of the solution, while the

furnace was slowly cooled (15 K/h) to room temperature to avoid thermal stresses.

Epitaxial layers with good optical quality were obtained with an average growth rate of 8.3 μm/h..

The chemical composition of the epitaxial layers, determined by Electron Probe Microanalysis (EPMA), was $RbTi_{0.973}Yb_{0.009}Nb_{0.018}OPO_4$. The Ba^{2+} concentration in the epitaxial layer was lower than the detection limit of this ion by EPMA. However, this ion was present in the epitaxial layers, since their refractive indices changed, as described below. The low level of Ba^{2+} incorporation in the RTP structure could be explained by the different ionic charge of the Ba^{2+} and Rb^+ ions and the different ionic radii of these two ions [9].

The refractive indices of the epitaxial layers and the substrates, as a function of the wavelength, were measured by the total internal reflection angle law. The light was coupled with a prism (Metricon prism coupler) using several laser sources. To optimize the coupling process, the epilayer was polished down to a thickness of 50 μm. The refractive indices obtained for the $RbTi_{0.973}Yb_{0.009}Nb_{0.018}OPO_4$ epitaxial layer with Ba^{2+} traces and those of the substrate at 632.8 nm are summarized in Table 1. The refractive indices of the epilayer are higher than those of the substrate along the y and z directions, indicating that this layer could support TM and TE propagation modes.

Table 1. Refractive indices of the Ba:Yb:Nb:RTP/RTP waveguide

Wavelength [nm]	n_x	n_y	n_z
532.0	1.805	1.822	1.921
632.8	1.788	1.802	1.896
770.0	1.776	1.787	1.875
780.4	1.775	1.788	1.873
790.0	1.774	1.786	1.873
820.4	1.772	1.786	1.869
840.9	1.771	1.785	1.867
971.0	1.766	1.779	1.861
980.6	1.765	1.777	1.862
989.2	1.765	1.776	1.861
1526.5	1.755	1.767	1.845

Refractive indices of the substrate			
Wavelength [nm]	n_x	n_y	n_z
632.8	1.789	1.801	1.888

From these refractive indexes we calculated the Sellmeier dispersion curves for these epilayers according to the expressions [10]:

$$n_i^2(\lambda) = A_i + \frac{B_i}{1 - \left(\frac{C_i}{\lambda}\right)^p} + \frac{D_i}{1 - \left(\frac{E_i}{\lambda}\right)^q} \qquad (1)$$

where i = x, y and z

The Sellmeier coefficients obtained are listed in Table 2. According to type II SHG, TM and TE fundamental infrared modes should propagate into the layer and TE second-harmonic modes should be generated. The PM condition for SHG is: $\frac{1}{2}[n_{TE}(\lambda_{pm}) + n_{TM}(\lambda_{pm})] - n_{TE}(\lambda_{pm}/2) = 0$

where $n_{TE}(\lambda_{pm})$ and $n_{TM}(\lambda_{pm})$ are the effective refractive indices for the TE and TM propagation modes at the phase-matching wavelength (λ_{pm}), respectively, and $n_{TE}(\lambda_{pm}/2)$ is the effective refractive index for the TE guided mode at the second-harmonic wavelength ($\lambda_{pm}/2$). [11]

Table 2. Sellmeier coefficients obtained by fitting the chromatic dispersion curves to the equations (1)

	A	B	C	D (nm)	E (nm)	p	q
n_x	2.3718	0.6979	0.2494	1.2900	13.0012	2.0012	1.9412
n_y	2.4081	0.7112	0.2481	0.8041	10.5332	2.0091	1.8981
n_z	2.3412	1.0592	0.2521	0.6771	10.1721	2.0112	1.8001

In order to prove these conditions, and demonstrate the propagation of the TM and TE modes in the waveguide, we polished the epitaxial layer down to 10 μm thickness. Figure 1 shows the dark mode spectrum in the TE polarization (electric field of the incident light parallel to the b crystallographic direction) obtained by the prism-film coupling technique, where only a propagation mode is observed. If the electric field of the incident light is parallel to the c crystallographic direction (TM polarization) we could observe five propagation modes into the 10 μm thickness epilayer. It is interesting to have only one TE propagation mode and a reduced number of TM propagation modes into the epilayer to have a better coupling among them and obtain a more efficient SHG process [12].
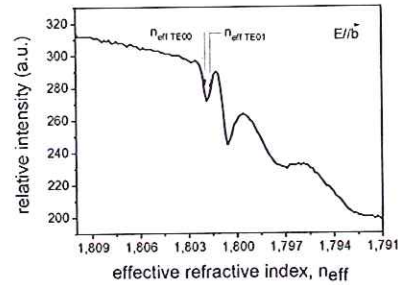

Fig. 1. Dark mode spectrum with TE polarization in a 10 μm Ba:Yb:Nb:RTP/RTP epitaxial layer at 632.8 nm

The type II PM curves in the a-b plane were obtained from the Sellmeier equations calculated for these epilayers, together with the phase matching condition and taking into account the Fresnel equation for biaxial crystals. The expression obtained was:

$$\frac{2}{\sqrt{\frac{\cos^2(\varphi)}{n_z^2(2\omega)} + \frac{\sin^2(\varphi)}{n_x^2(2\omega)}}} = n_z(\omega) + \frac{1}{\sqrt{\frac{\cos^2(\varphi)}{n_y^2(\omega)} + \frac{\sin^2(\varphi)}{n_x^2(\omega)}}} \qquad (2)$$

where φ is the angle of light propagation into the waveguide in the a-b plane, and n_x, n_y and n_z are the refractive indices with the electric field parallel to the a, b and c crystallographic directions, respectively. Figure 2 shows the phase matching curve for type II PM SHG

calculated from these equations. From this figure we can observe that the range of wavelengths for which type II PM can be obtained in these samples is larger than in undoped RTP [10] and the SHG wavelengths extend towards the blue region.
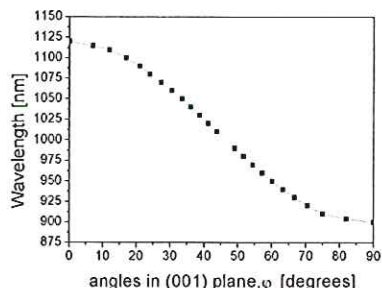

Fig. 2. Calculated phase-matching curve for type II SHG in Ba:Yb:Nb:RTP/RTP epitaxial layer

To investigate the single pass type II PM SHG, we polished the faces perpendicular to the *a* crystallographic direction. We used an OPO to couple the light that propagate along this direction into the waveguide using microscope objectives and tune the wavelength to obtain the maximum efficiency of SHG for propagation along this direction. The waveguide length was 1.1 cm. An achromatic half-wave plate was placed between the laser source and the sample at an angle of $22.5°$ to ensure the type II SHG. The guided green light obtained by SHG was observed with a CCD camera and is shown in Figure 3, which also shows the wavelength spectrum in the Figure inset. The most efficient SHG was obtained for a fundamental wavelength of the IR light coupled to the epilayer of 1125 nm, with 0.008 mJ per pulse (10 ns per pulse), a little above the theoretical value but close to it, whereas the second harmonic radiation generated was in the green region (562.5 nm) (see inset in Figure 3). After filtering the output radiation with an IR filter, we measured the second harmonic power with a power meter. The efficiency of type II PM SHG, calculated using the expression $\eta = P_{2\omega}/P_\omega$, was 0.69.
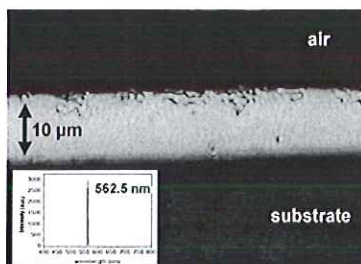

Fig. 3. Type II SHG in a Ba:Yb:Nb:RTP/RTP epitaxial layer with the fundamental radiation of 1125 nm and SH radiation of 562.5 nm. Inset: wavelength spectrum with maximum at 562.5 nm

To summarize, we have shown a highly efficient method of obtaining type II PM SHG on Ba:Yb:Nb:RTP/RTP waveguides. When the epitaxial layer was co-doped with Ba^{2+} we obtained TM and TE polarization modes confined in the waveguide, which is essential for type II PM SHG interactions. The PM curve calculated from the Sellmeier equations obtained for these epilayers showed that the wavelengths that can be doubled ranged from 900 to 1125 nm, a range that includes the Yb^{3+} emission in theses materials. We could confirm experimentally the upper limit of this curve, indicating that self-frequency doubling could be obtained in these epilayers in the future.

[1] P. A. Thomas, S.C. Mayo and B.E. Watts, *Acta Crystallog.* B48, 401-407 (1992).

[2] C. Zumsteg, C.J. Bierlein and T.E. Gier, *J. Appl. Phys.* 47, 4980-4985 (1976).

[3] Y.S. Oseledchik, S.P. Belokrys, V.V. Osadchuk, A.L. Prosvirnin, A.F. Selevich, V.V. Starshenko, K.V. Kuzemchenko, *J. Cryst. Growth* 125, 639-643 (1992).

[4] X. Mateos, V. Petrov, A. Peña, A.; J.J. Carvajal, M. Aguiló, F. Díaz, P. Segonds and B. Boulanger, *Opt. Lett.* 32, 1929-1931 (2007).

[5] J. Cugat, R. Solé, M.C. Pujol, J.J. Carvajal, X. Mateos, F. Díaz, M. Aguiló, *Opt. Mater.* 32, 1648-1651 (2010).

[6] N. Yamada, Y. Yamamoto, *J. J. of Appl. Phys.* 33, 6572-6576 (1994).

[7] J. Cugat, R. Solé, J. J. Carvajal, M. C. Pujol, X. Mateos, F. Díaz, M. Aguiló, *Cryst. Eng Comm.* DOI: 10.1039/C0CE00647E (accepted 26th November 2010, in press).

[8] R. Solé, V. Nikolov, A. Vilalta, J.J. Carvajal, J. Massons, Jna. Gavaldà, M. Aguiló, F. Díaz, *J. Mater. Res.* 17(3), 563-569 (2002).

[9] R.D. Shannon, *Acta Cryst.* A3, 751-767 (1976).

[10] Y. Guillen, B. Ménaert, J.P. Fève, P. Segonds, J. Douady, B. Boulanger, O. Pacaud, *Opt. Mater.* 22, 155-162 (2003).

[11] W. P. Risk, T. R. Gosnell, A. V. Nurmikko, *Compact blue-green lasers*, Cambridge University Press (2003).

[12] W. P. Risk, S. D. Lau, R. ; Fontana, L. Lane, Ch. Nadier, *Appl. Phys. Lett.* 63 (10), 1301-1303 (1993).

[1] P. A. Thomas, S.C. Mayo and B.E. Watts, "Crystal structures of $RbTiOAsO_4$, $KTiO(P_{0.58},As_{0.42})O_4$, $RbTiOPO_4$ and $(Rb_{0.465},K_{0.535})TiOPO_4$, and analysis of pseudosymmetry in crystals of the $KTiOPO_4$ family" *Acta Crystallog.* B48, 401-407 (1992).

[2] C. Zumsteg, C.J. Bierlein and T.E. Gier, "A new nonlinear optical material $K_xRb_{1-x}TiOPO_4$" *J. Appl. Phys.* 47, 4980-4985 (1976).

[3] Y.S. Oseledchik, S.P. Belokrys, V.V. Osadchuk, A.L. Prosvirnin, A.F. Selevich, V.V. Starshenko, K.V. Kuzemchenko, "Growth of $RbTiOPO_4$ single crystals from phosphate systems" *J. Cryst. Growth* 125, 639-643 (1992).

[4] X. Mateos, V. Petrov, A. Peña, A.; J.J. Carvajal, M. Aguiló, F. Díaz, P. Segonds and B. Boulanger, "Laser operation of Yb^{3+} in the acentric $RbTiOPO_4$ codoped with Nb^{5+} " *Opt. Lett.* 32, 1929-1931 (2007)

[5] J. Cugat, R. Solé, M.C. Pujol, J.J. Carvajal, X. Mateos, F. Díaz, M. Aguiló, "Waveguiding demonstration on $Yb:Nb:RbTiOPO_4/RbTiOPO_4(001)$ epitaxies grown by LPE" *Opt. Mater.* 32, 1648-1651 (2010).

[6] N. Yamada, Y. Yamamoto, "Refractive index profiles of $KTiOPO_4$ ion-exchanged waveguides and effect of barium ion" *J. J. of Appl. Phys.* 33, 6572-6576 (1994).

[7] J. Cugat, R. Solé, J. J. Carvajal, M. C. Pujol, X. Mateos, F. Díaz, M. Aguiló, "Crystal growth and characterization of $RbTi_{1-x-y}Yb_xNb_yOPO_4/RbTiOPO_4(001)$ nonlinear optical epitaxial layers" *Cryst. Eng Comm.* DOI: 10.1039/C0CE00647E (accepted 26th November 2010, in press).

[8] R. Solé, V. Nikolov, A. Vilalta, J.J. Carvajal, J. Massons, Jna. Gavaldà, M. Aguiló, F. Díaz, "Growth of $KTiOPO_4$ films on $KTi_{1-x}Ge_xOPO_4$ substrates by liquid-phase epitaxy" *J. Mater. Res.* 17(3), 563-569 (2002).

[9] R.D. Shannon, "Revised effective ionic radii sytematic studies of interatomic distances in halides and chalcogenides" *Acta Cryst.* A3, 751-767 (1976).

[10] Y. Guillen, B. Ménaert, J.P. Fève, P. Segonds, J. Douady, B. Boulanger, O. Pacaud, "Crystal growth and refined Sellmeier equations over the complete transparency range of $RbTiOPO_4$" *Opt. Mater.* 22, 155-162 (2003).

[11] W. P. Risk, T. R. Gosnell, A. V. Nurmikko, *Compact blue-green lasers*, Cambridge University Press (2003).

[12] W. P. Risk, S. D. Lau, R.; Fontana, L. Lane, Ch. Nadier, "Type-II second-harmonic generation and sum-frequency mixing in uniform $KTiOPO_4$ channel waveguides" *Appl. Phys. Lett.* 63 (10), 1301-1303 (1993).